No Difference in Ligamentous Strain or Knee Kinematics Between Rectangular or Cylindrical Femoral Tunnels During Anatomic ACL Reconstruction With a Bone–Patellar Tendon–Bone Graft

Timothy A. Burkhart,* PhD, Takashi Hoshino,† MD, Lachlan M. Batty,‡ MBBS, Alexandra Blokker,§ MESc, Philip P. Roessler,‖ MD, Rajeshwar Sidhu,† MBBS, MSc, MS(Ortho), Maria Drangova,¶ PhD, David W. Holdsworth,¶ PhD, Ivailo Petrov,¶ PhD, Ryan Degen,† MD, and Alan M. Getgood,†# MD

Investigation performed at the Fowler Kennedy Sports Medicine Clinic, Western University, London, Ontario, Canada

Background: As our understanding of anterior cruciate ligament (ACL) anatomy has evolved, surgical techniques to better replicate the native anatomy have been developed. It has been proposed that the introduction of a rectangular socket ACL reconstruction to replace a ribbon-shaped ACL has the potential to improve knee kinematics after ACL reconstruction.

Purpose: To compare a rectangular femoral tunnel (RFT) with a cylindrical femoral tunnel (CFT) in terms of replicating native ACL strain and knee kinematics in a time-zero biomechanical anatomic ACL reconstruction model using a bone–patellar tendon–bone (BTB) graft.

Study Design: Controlled laboratory study.

Methods: In total, 16 fresh-frozen, human cadaveric knees were tested in a 5 degrees of freedom, computed tomography–compatible joint motion simulator. Knees were tested with the ACL intact before randomization to RFT or CFT ACL reconstruction using a BTB graft. An anterior translation load and an internal rotation moment were each applied at 0°, 30°, 60°, and 90° of knee flexion. A simulated pivot shift was performed at 0° and 30° of knee flexion. Ligament strain and knee kinematics were assessed using computed tomography facilitated by insertion of zirconium dioxide beads placed within the substance of the native ACL and BTB grafts.

Results: For the ACL-intact state, there were no differences between groups in terms of ACL strain or knee kinematics. After ACL reconstruction, there were no differences in ACL graft strain when comparing the RFT and CFT groups. At 60° of knee flexion with anterior translation load, there was significantly reduced strain in the reconstructed state ([mean ±standard deviation] CFT native, 2.82 ± 3.54 vs CFT reconstructed, 0.95 ± 2.69; RFT native, 2.77 ± 1.71 vs RFT reconstructed, 1.40 ± 1.76) independent of the femoral tunnel type. In terms of knee kinematics, there were no differences when comparing the RFT and CFT groups. Both reconstructive techniques were mostly effective in restoring native knee kinematics and ligament strain patterns as compared with the native ACL.

Conclusion: In the time-zero biomechanical environment, similar graft strains and knee kinematics were achieved using RFT and CFT BTB ACL reconstructions. Both techniques appeared to be equally effective in restoring kinematics associated with the native ACL state.

Clinical Relevance: These data suggest that in terms of knee kinematics and graft strain, there is no benefit in performing the more technically challenging RFT as compared with a CFT BTB ACL reconstruction.

Keywords: anterior cruciate ligament reconstruction; rectangular socket; biomechanics; knee kinematics

The Orthopaedic Journal of Sports Medicine, 9(6), 23259671211009523
DOI: 10.1177/23259671211009523

In the evolution of anterior cruciate ligament (ACL) reconstruction (ACLR), early nonanatomic reconstructive procedures have been replaced with modern intra-

articular reconstructions.[12] These techniques aim to replicate the native ACL anatomy, improve knee stability, and avoid overconstraint by restoring the native ACL dimensions, collagen orientation, and insertion sites.[15]

As ACLR techniques have continued to be refined, descriptions of the native ACL anatomy have also continued to evolve.[12,15,22,23,34,36] The double-bundle concept proposed that the anteromedial (AM) and posterolateral (PL) bundles of the ACL work synergistically to control tibiofemoral motion, with the AM bundle primarily resisting anterior tibial translation and the PL bundle providing rotational stability.[1,8,11,18,29] The macroscopic morphology of the ACL has more recently been described as a flat, ribbon-like ligament.[36] When the surface membrane of the ACL was removed, discrete bundles were not identified, thus challenging the previously held notion of AM and PL bundles. As such, a linear ACL femoral origin arising in continuity with the posterior femoral cortex was described.[36] With a focus on replicating these anatomic descriptions, commercially available reconstructive techniques have been developed, typically with hamstring or quadriceps tendon autograft.[1,8,11,24,29,35]

Bone–patellar tendon–bone (BTB) autograft is another common graft choice for ACLR with proposed advantages including bone-to-bone healing, reduced postoperative pivot shift, and lower failure rates in some series.[28,42] The BTB graft is also favorable for reconstructing a ribbon-like ACL because of its flat morphology. Some have proposed it as a means of replicating a functional double-bundle reconstruction using a single graft.[10,26,32] An important factor in successful reconstruction is accurate positioning of the tendinous portion of the graft. Traditionally, cylindrical tunnels and bone dowels have been utilized in BTB ACLRs. However, with cylindrical preparations, the tunnel aperture may not represent the functional aperture, as the patellar tendon is positioned eccentrically on the bone block. Therefore, the position of the tendon can vary based on positioning within the socket. This can be technically difficult to control with precision during surgery. While it has recently been demonstrated that bone block orientation within the femoral tunnel affects native ACL femoral footprint coverage,[2] the editorial accompanying the paper highlighted that the effects of graft orientation on knee kinematics remain unclear.[16] It has been proposed that rectangular tunnels in ACLR may be a way to better control graft orientation and positioning.[30-33]

The purpose of the current study was to compare an anatomic rectangular femoral tunnel (RFT) ACLR with an anatomic cylindrical femoral tunnel (CFT) ACLR for replicating native ACL strain characteristics and knee kinematics in a cadaveric biomechanical model. We hypothesized that there would be no difference between RFT and CFT ACLRs in graft strain or knee kinematics in response to clinically relevant load applications.

METHODS

Specimen Preparation

A total of 16 fresh-frozen, cadaveric knee specimens with a mean (± standard deviation) age of 69 ± 9 years (range, 48-87 years), comprising 8 male and 5 female specimens, were procured for use in this study (United Tissue Network). The use of deidentified specimens does not require research ethics board review at our institution; however, all research, tissue storage, and tissue disposal protocols were reviewed and approved by the United Tissue Network, which is accredited by the American Association of Tissue Banks. Once thawed, the specimens were sectioned to obtain a femoral and tibial length of 20 cm each, measured from the joint center. All supporting soft tissues surrounding the joint were preserved, with special care not to disrupt the joint capsule and ligamentous structures. The distal tibia was potted within a 5.0 cm–diameter section of acrylonitrile-butadiene-styrene tubing and secured in place using dental cement (Denstone Dental Cement; Hereaus Holdings GmbH). The specimen was then inverted and held in extension while the proximal femur was potted into a section of 7.7 cm–diameter acrylonitrile-butadiene-styrene, with approximately 10 N of compressive load applied through the tibia during this process to maintain the knee's native mechanical angle.[5] The specimens were inspected visually and arthroscopically and examined clinically to exclude previous ACL or other ligamentous injury, osteoarthritis, or meniscal pathology.

To track the deformation of the ACL in response to physiologically relevant loading, 14 small-diameter (800 μm) zirconium dioxide beads (Boca Bearings) were inserted into the native ACL and BTB grafts (Figure 1). For the native

[#]Address correspondence to Alan M. Getgood, MD, Fowler Kennedy Sports Medicine Clinic, Western University, London, Ontario, Canada (email: algetgood@gmail.com) (Twitter: @FKSMC_Getgood).
[*]Mechanical and Materials Engineering, Western University, London, Ontario, Canada.
[†]Fowler Kennedy Sports Medicine Clinic, Western University, London, Ontario, Canada.
[‡]St. Vincent's Hospital, Melbourne, Victoria, Australia.
[§]Biomedical Engineering, Western University, London, Ontario, Canada.
[‖]University Hospital Bonn, Bonn, Germany.
[¶]Robarts Research Institute, Western University, London, Ontario, Canada.
Final revision submitted November 24, 2020; accepted January 4, 2021.
One or more of the authors has declared the following potential conflict of interest or source of funding: This study was supported by an unrestricted research grant from Smith & Nephew, an Ontario Research Fund (Research Excellence) grant, and a CIHR Foundation grant (FDN No. 148474). T.A.B. receives salary support from Smith & Nephew. A.M.G. has received consulting fees from Smith & Nephew, Olympus, and Ossur; royalties from Smith & Nephew and Gramont; and research support from Smith & Nephew and Ossur. AOSSM checks author disclosures against the Open Payments Database (OPD). AOSSM has not conducted an independent investigation on the OPD and disclaims any liability or responsibility relating thereto.
Ethical approval was not sought for the present study.

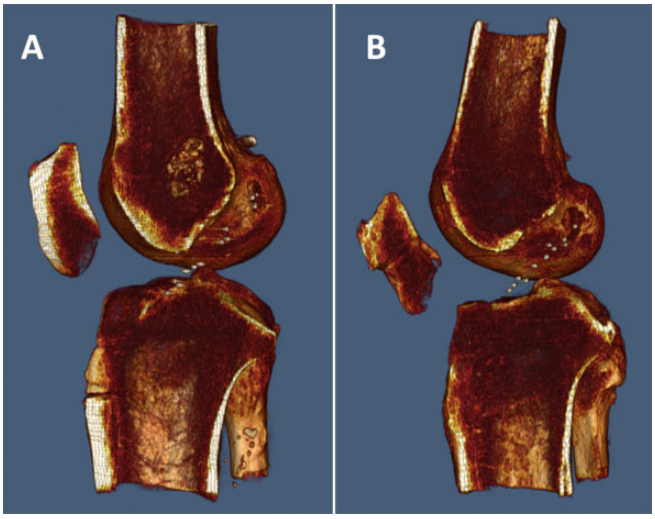

Figure 1. Medial view of 3-dimensional computed tomography reformats. The medial femoral condyle and medial tibial plateau have been subtracted after (A) rectangular and (B) cylindrical femoral tunnel anterior cruciate ligament (ACL) reconstruction. Note in both panels the zirconium dioxide beads within the substance of the ACL graft that were used to assess ligamentous strain.

ACL, the femur was secured in an arthroscopic extremity holder (Model 1650 Sawbones; Pacific Research Laboratories), and the beads were inserted arthroscopically using an 18-gauge needle (BD Precision Glide). The beads were arranged in 2 columns, allowing for the calculation of both axial and transaxial strain, with an interbead distance of approximately 3 mm; 4 were positioned at the femoral footprint, 6 were positioned in the midsubstance, and 4 were positioned in the tibial footprint.[4] This bead tracking method to calculate tissue strain has been shown not to affect the material properties of the tissue, and the beads do not migrate within the tissue when subjected to cyclic loading.[6]

Experimental Setup

Once potted, the intact specimens were secured within a custom-designed 5 degrees of freedom, computed tomography (CT)–compatible joint motion simulator (Figure 2) that has previously been described.[5] The simulator allows passive control over knee flexion, while active control over compression/distraction, anterior/posterior translation, internal/external rotation, and varus/valgus rotation is achieved using the actuating components of the simulator. The steady-state error of the simulator has been shown to range from 0% (internal rotation) to 0.11% (anterior translation).[6] The center of the knee joint was aligned with the center of the CT scanner bore (80 kVp, 50 mA; 745 projections acquired at 0.48° angular increments around the sample in 26 seconds; anisotropic voxels measuring 0.207 × 0.207 mm in-plane, and 0.415 mm out-of-plane; O-Arm; Medtronic).

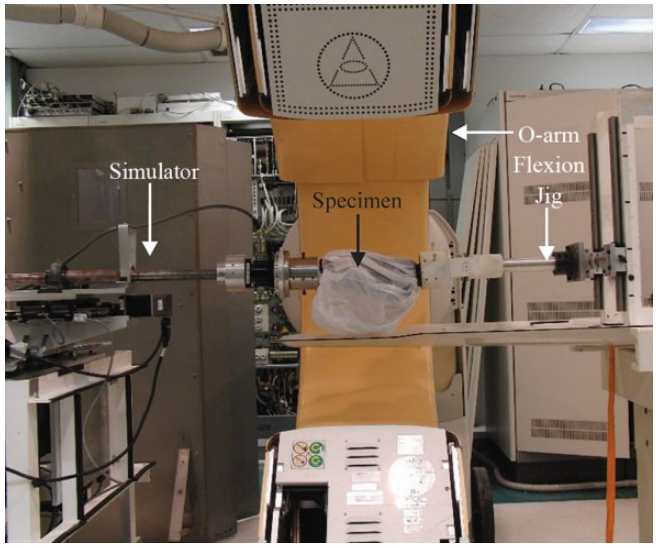

Figure 2. Side view of the experimental setup of a specimen, at 0° of flexion, within the joint simulator centered in the O-arm's field of view. The O-arm is open to view the specimen that is wrapped in a plastic bag to adhere to biohazard protocols.

Sectioning and Surgical Protocols

The specimens were initially tested in the ACL intact state. Next, the ACL was sectioned, and all remaining remnants were removed arthroscopically. The specimens were then randomly assigned to undergo ACLR using a BTB graft with either a CFT (n = 8) or an RFT (n = 8). Each reconstruction was tested under the same protocol as that for the intact ACL condition (described below). For all specimens, an anatomic transportal single-bundle ACLR was performed using an ipsilateral patellar tendon autograft.

Graft Preparation

Using a longitudinal midline skin incision, we harvested a 10 mm–wide strip of patellar tendon with a 20 × 10–mm bone block from the patella and a 25 × 10–mm bone block from the proximal tibia. For the CFT graft, the patellar bone block was fashioned into a 9 mm–diameter × 20 mm–long cylindrical bone dowel, and the tibial bone block was fashioned into a 10 mm–diameter × 25 mm–long bone dowel. A No. 5 Ethibond suture (Ethicon Inc) was passed through a 1.8-mm drill hole on the patellar bone block for femoral passage. Two tension sutures (No. 5 Ethibond) were placed through 2 × 1.8–mm drill holes on the tibial bone block. For the RFT graft, the patellar bone plug was also utilized for the femoral side. This was shaped into a rectangular 5 mm–thick × 10 mm–wide × 20 mm–long bone block. The tibial bone block was compressed into a 10 mm × 25 mm cylindrical dowel using 2 No. 5 Ethibond tensioning sutures. Fourteen zirconium dioxide beads were inserted into each of the grafts using an 18-gauge needle (BD Precision Glide) in the same pattern that was used for the intact ACL.

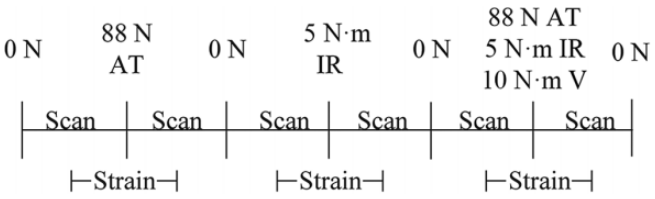

Figure 3. A schematic representation of the loading and scanning protocol. This was repeated at each of the 4 knee flexion angles (0°, 30°, 60°, 90°) and for both conditions (intact and anterior cruciate ligament reconstruction). The strains were calculated using the images from the loaded and the preceding zero-load states. AT, anterior translation; IR, internal rotation.

Creation of Bone Tunnels/Sockets

For the CFT, placement was guided by the ACL remnant and identification of the lateral intercondylar and the bifurcate ridge. The midpoint between AM and PL bundles was targeted and confirmed using visualization from the AM portal. The knee was flexed to 140°, and a 25 mm–depth socket was created using a 10-mm cannulated reamer over a Beath pin from an accessory medial portal (Figure 1).

For the RFT, a similar tunnel position was targeted using the ACL femoral remnant as a secondary check to confirm anatomic placement (Figure 1). The RFT cannulated guide (Smith & Nephew Inc) was introduced through an accessory medial portal. A Beath pin was placed into the central hole with the knee in deep flexion. The rectangular guide was aligned parallel to the intercondylar ridge. Two further Beath pins were inserted into the more proximal and distal holes of the guide, and the central pin was removed. The remaining Beath pins were then overdrilled using a 4.5-mm drill (Smith & Nephew) to a depth of 20 mm. The central pin was reinserted and drilled through to the far lateral cortex. The central pin was then overdrilled using the 4.5-mm drill to the far lateral cortex. The cannulated dilator was then inserted into the three 4.5-mm drill holes to a depth of 20 mm, creating a rectangular socket. The dilator was removed, and a passing suture placed.

Tibial tunnel preparation for both groups was performed using a tip aimer tibial guide (Smith & Nephew) that was set to 50° and placed in the middle of the residual tibial stump. This was cross-referenced with the anterior horn of the lateral meniscus and the medial tibial spine and viewed from the anterolateral portal at 90° of flexion and in extension to confirm appropriate placement. A 10-mm cannulated cylindrical reamer was used to drill over the wire. Femoral and tibial tunnel positions were subsequently assessed using 3-dimensional CT reconstructions using the Bernard and Hertel quadrant method.[3,9,14,20]

Graft Passage and Fixation

For both reconstructive techniques, the graft was passed from the tibial tunnel into the femoral socket. For the CFT reconstruction, the cancellous bone side of the dowel was positioned on the shallow aspect of the femoral tunnel, and the patellar tendon side of the graft was positioned on the deep aspect of the femoral tunnel so that fibers would run parallel with the intercondylar ridge. For the RFT group, the rectangular bone plug was kept with its cancellous bone surface maintained anteriorly. In both instances, the

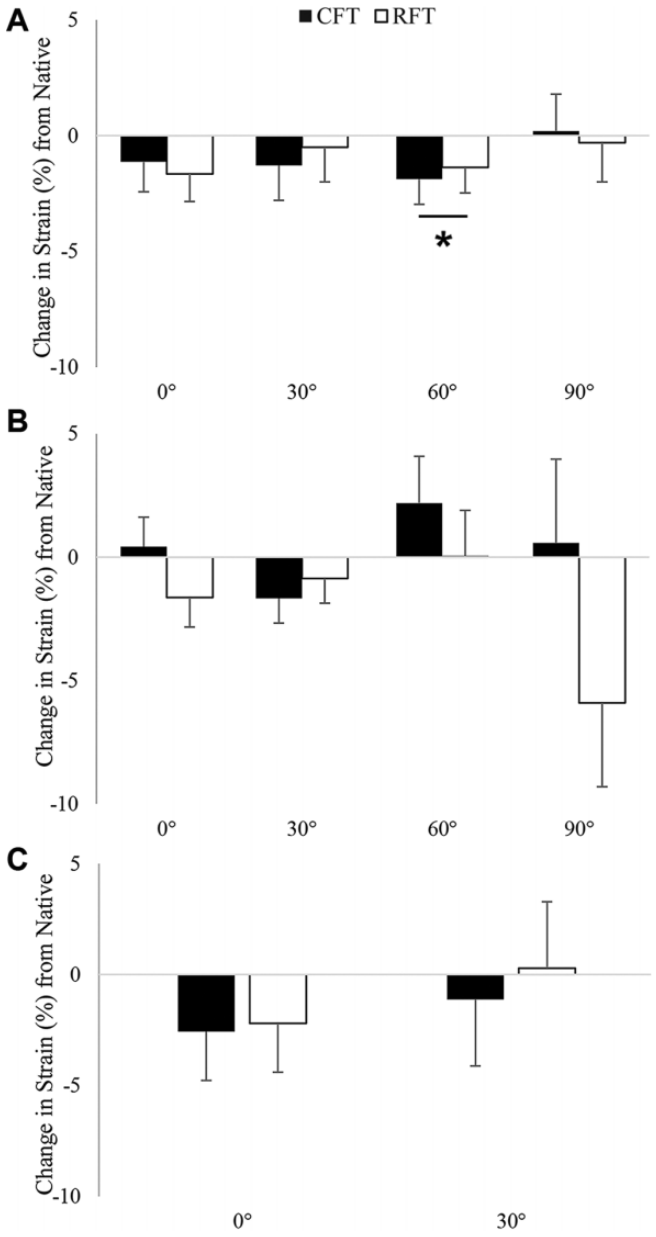

Figure 4. The change in strain at the reconstructed state compared with the native state in response to (A) an 88-N anterior translation load, (B) a 5-N·m internal rotation moment, and (C) a simulated pivot shift (88-N anterior translation, 5-N·m internal rotation moment, and 10-N·m valgus rotation moment). *Statistically significant difference between the native and reconstructed states independent of reconstruction type ($P < .05$). CFT, cylindrical femoral tunnel; RFT, rectangular femoral tunnel.

TABLE 1
ACL Strain Between the CFT and RFT Groups by Native and Reconstructed State Across Flexion Angles and Loading Protocols.[a]

Variable	Strain, %		*P* Value (ES)
	Native State	Reconstructed State	
Anterior translation			
0° of flexion			
CFT	2.02 ± 1.12 (–0.3 to 4.4)	0.89 ± 1.31 (0 to 1.8)	.39 (0.76)
RFT	2.82 ± 4.22 (0.5 to 5.2)	1.17 ± 1.64 (0.3 to 2.1)	.22 (0.58)
P value (ES)	.61 (0.26)	.64 (0.19)	
30° of flexion			
CFT	3.41 ± 6.11 (0.8 to 6.1)	2.12 ± 3.57 (0.3 to 4.0)	.40 (0.18)
RFT	2.22 ± 2.40 (–0.4 to 4.9)	1.72 ± 1.02 (–0.1 to 3.6)	.74 (0.59)
P value (ES)	.51 (0.26)	.75 (0.15)	
60° of flexion			
CFT	2.82 ± 3.54 (0.8 to 4.8)[b]	0.95 ± 2.69 (–0.2 to 2.1)	.10 (0.58)
RFT	2.77 ± 1.71 (0.8 to 4.8)[b]	1.40 ± 1.76 (0.2 to 2.5)	.21 (**0.89**)
P value (ES)	.97 (0.02)	.58 (0.19)	
90° of flexion			
CFT	1.06 ± 7.58 (–0.2 to 3.9)	1.31 ± 2.42 (–0.1 to 2.7)	.89 (0.05)
RFT	1.20 ± 5.00 (–0.2 to 4.2)	0.85 ± 1.93 (–0.6 to 2.3)	.84 (0.08)
P value (ES)	.94 (0.02)	.63 (0.21)	
Internal rotation			
0° of flexion			
CFT	0.61 ± 2.49 (–1.8 to 3.0)	1.04 ± 1.41 (0.3 to 1.8)	.71 (0.19)
RFT	2.76 ± 3.79 (0.4 to 5.2)	1.12 ± 2.02 (0.4 to 1.9)	.18 (0.47)
P value (ES)	.20 (0.67)	.87 (0.04)	
30° of flexion			
CFT	–0.07 ± 3.04 (–2.3 to 2.2)	–1.74 ± 5.16 (–4.1 to 0.7)	.12 (0.41)
RFT	0.86 ± 3.58 (–1.4 to 3.1)	0.002 ± 1.17 (–2.4 to 2.4)	.42 (0.34)
P value (ES)	.54 (0.28)	.29 (0.46)	
60° of flexion			
CFT	–2.94 ± 4.75 (–6.4 to 0.5)	–0.75 ± 4.81 (–3.6 to 2.0)	.28 (0.54)
RFT	–1.67 ± 4.94 (–5.1 to 1.8)	–1.67 ± 2.14 (–4.5 to 1.1)	.99 (0.01)
P value (ES)	.60 (0.26)	.63 (0.24)	
90° of flexion			
CFT	–2.24 ± 3.44 (–4.4 to –0.1)	–1.66 ± 3.62 (–8.9 to 5.6)	.87 (0.15)
RFT	–1.93 ± 2.78 (–4.1 to 0.2)	–7.84 ± 14.66 (–15.1 to –0.6)	.10 (0.59)
P value (ES)	.83 (0.10)	.22 (0.58)	
Pivot shift			
0° of flexion			
BTB	3.58 ± 6.39 (0 to 7.1)	1.01 ± 2.64 (–0.6 to 2.6)	.26 (0.49)
RFT-BTB	3.55 ± 4.11 (0 to 7.1)	1.35 ± 1.47 (–0.2 to 2.9)	.34 (0.64)
P value (ES)	.99 (0.01)	.75 (0.15)	
30° of flexion			
BTB	2.85 ± 9.63 (–1.6 to 7.3)	1.73 ± 4.51 (–2.4 to 5.9)	.70 (0.11)
RFT-BTB	3.44 ± 3.91 (–1.0 to 7.9)	3.72 ± 6.43 (–0.4 to 7.8)	.72 (0.06)
P value (ES)	.84 (0.08)	.48 (0.36)	

[a]Data are reported as mean ± SD (95% CI) unless otherwise indicated. Bold text indicates large pairwise Cohen δ effect size (ES). BTB, bone–patellar tendon–bone; CFT, cylindrical femoral tunnel; RFT, rectangular femoral tunnel.
[b]$P < .05$ between the native and reconstructed states, independent of reconstruction type.

suture was tied over an Endobutton (Smith & Nephew) on the lateral femoral cortex, accessed through a small skin incision. After femoral fixation, the graft was rotated within the tibial tunnel under arthroscopic visualization to replicate an AM and PL positioning of the patellar tendon within the tibial tunnel aperture. The knee was then cycled 20 times through flexion and extension with 80 N of tension applied to the tibial-sided graft sutures using a fish-scale tensioning device. The graft was then fixed with 80 N of tension and the knee flexed to 15°. Tibial fixation for both reconstructive techniques consisted of a 7 mm × 25 mm cannulated PEEK interference screw (Biosure PK; Smith & Nephew) placed at the anterolateral aspect of the tibial tunnel.

Loading and Imaging Protocols

Before testing at each condition, 10 internal rotation and 10 anterior translation precondition cycles were applied to the

TABLE 2
Anterior Translation and Internal Rotation Between the CFT and RFT Groups by Native and Reconstructed State Across Flexion Angles and Loading Protocols[a]

Variable	Native State	Reconstructed State	*P* Value (ES)
Anterior translation, mm			
0° of flexion			
CFT	2.3 ± 1.0 (1.0 to 3.6)	2.3 ± 2.8 (0.4 to 4.2)	.95 (0.03)
RFT	3.4 ± 2.3 (2.1 to 4.7)	2.9 ± 2.2 (1.0 to 4.8)	.50 (0.40)
P value (ES)	.22 (0.64)	.65 (0.23)	
30° of flexion			
CFT	3.6 ± 3.3 (1.2 to 6.0)	2.9 ± 1.8 (1.3 to 4.6)	.62 (0.21)
RFT	3.3 ± 2.6 (1.1 to 5.6)	2.9 ± 2.2 (1.3 to 4.5)	.74 (0.53)
P value (ES)	.85 (0.10)	.98 (0.02)	
60° of flexion			
CFT	4.3 ± 2.0 (2.9 to 5.7)	5.6 ± 3.2 (3.3 to 7.9)	.24 (0.61)
RFT	3.4 ± 1.7 (2.0 to 4.8)	4.7 ± 2.9 (2.4 to 7.0)	.24 (0.61)
P value (ES)	.35 (0.48)	.57 (0.29)	
90° of flexion			
CFT	3.5 ± 3.0 (1.7 to 5.3)	3.5 ± 2.4 (0.5 to 6.4)	.98 (0.01)
RFT	1.7 ± 1.3 (–0.1 to 3.4)	5.4 ± 4.9 (2.5 to 8.3)	.06 (**0.99**)
P value (ES)	.14 (0.79)	.34 (0.50)	
Internal rotation, deg			
0° of flexion			
CFT	11.2 ± 8.3 (4.8 to 17.7)	9.6 ± 9.2 (4.2 to 15.0)	.53 (0.27)
RFT	11.3 ± 8.8 (4.8 to 17.8)	10.4 ± 4.4 (5.0 to 15.9)	.71 (0.24)
P value (ES)	.98 (0.01)	.82 (0.11)	
30° of flexion			
CFT	15.5 ± 11.3 (7.2 to 23.8)	13.7 ± 10.1 (7.6 to 19.8)	.89 (0.49)
RFT	14.9 ± 10.5 (6.7 to 23.2)	14.6 ± 5.3 (8.4 to 20.7)	.52 (0.06)
P value (ES)	.92 (0.05)	.84 (0.11)	
60° of flexion			
CFT	12.2 ± 7.4 (6.8 to 17.6)	16.2 ± 6.2 (12.2 to 20.3)	.14 (**0.98**)
RFT	14.4 ± 6.7 (9.0 to 19.7)	12.5 ± 4.3 (8.4 to 16.5)	.47 (0.04)
P value (ES)	.55 (0.30)	.18 (0.70)	
90° of flexion			
CFT	9.3 ± 7.1 (4.9 to 12.8)	13.1 ± 9.7 (6.2 to 20.0)	.32 (0.52)
RFT	5.6 ± 4.1 (1.2 to 10.0)	9.4 ± 8.4 (2.5 to 16.3)	.31 (0.56)
P value (ES)	.22 (0.64)	.43 (0.40)	

[a]Data are reported as mean ± SD (95% CI) unless otherwise indicated. Bold text indicates large pairwise Cohen δ effect size (ES). CFT, cylindrical femoral tunnel; RFT, rectangular femoral tunnel.

specimens at 0.25 Hz. After preconditioning and with the knee in 0° of flexion, the active axes were set to zero load, and a baseline scan was taken. After the baseline scan, the knee was loaded, and a second scan was taken when the target load was achieved. A baseline scan was taken before each of the separate loading conditions to minimize variability in the strain calculations (see "Strain Calculation" section) (Figure 3). Each scan was initiated within seconds of achieving the target load and took approximately 26 seconds to complete. Intact and reconstructed knees were tested under 3 simulated conditions: (1) isolated 88-N anterior translation load (25 N/s); (2) isolated 5-N·m internal rotation moment (1 N·m/s); and (3) a simulated pivot shift consisting of a combined 88-N anterior translation, 5-N·m internal rotation moment, and 10-N·m valgus moment (2 N·m/s). For all loading conditions, a 10-N axial compression load was applied. The isolated loading conditions were applied to the specimen at 0°, 30°, 60°, and 90° of knee flexion, while the simulated pivot shift was tested at 0° and 30° of flexion only.

Strain Calculation

Beam-hardening correction and metal-artifact reduction were applied in postprocessing to the CT images, and they were rescaled into Hounsfield units. The centroid location (x, y, z coordinate) of each bead was computed using custom-developed software. A second custom-designed software program (standard toolkits; MATLAB R2017b; MathWorks) calculated the graft strain by comparing the Euclidean distance between the beads in the femoral insertion and the tibial insertion before (baseline scan) and after an applied load.[4,5] The average strain between the 2 columns was used in subsequent analyses. It should be noted again that before each loading condition, a baseline scan was performed, and this served as each loaded condition's initial state (Figure 3). This strain measurement method (at 5-mm interbead distances and 250-μm CT resolution) is capable of measuring strain as low as 0.007 strain with root-mean-square errors that range

from 0.001 strain to 0.005 strain.[7] This method has shown excellent repeatability in measuring tissue strain (intraclass correlation coefficients, 0.962-1.00 across 5 cycles).[4]

Knee Kinematic Assessment

Using the CT images, a set of anatomic landmarks were selected to create tibial and femoral coordinate systems. The relevant kinematics were then calculated using the Grood and Suntay method as recommended by the International Society of Biomechanics.[17,41] This method has been shown to have low interrater error that has a minimal effect on the joint kinematics.[5]

Statistical Analysis

An independent *t* test was used to determine whether there were statistically significant differences between the positions of the bone tunnels between the CFTs and RFTs. A 3-way (2 states [intact vs reconstructed] × 4 regions [tibia insertion vs proximal midsubstance vs distal midsubstance vs femoral insertion] × 2 reconstruction methods [CFT vs RFT]), mixed repeated-measures analysis of variance was conducted to determine the effect of graft type on the strain magnitude. The state was the within-specimen variable, and the type of reconstruction and region were the between-specimen variables. Separate analyses of variance were performed for each of the loading conditions and for each flexion angle. The overall partial η^2 effect sizes were calculated (large effect, >0.14), while pairwise effect sizes were assessed using Cohen δ (large effect, >0.80).[21] All post hoc testing was accomplished using a Bonferroni adjustment, and α was set at .05 for all statistical tests (IBM SPSS Version 25).

RESULTS

Tunnel Positioning

When comparing the mean (± standard deviation) CFT and RFT femoral tunnel placement as measured using the Bernard and Hertel quadrant method, there was no significant difference in tunnel position for mean femoral tunnel depth (26.75% ± 5.99% vs 23.50% ± 3.11%; $P = .20$) or height (29.75% ± 4.80% vs 26.38% ± 8.09%; $P = .33$). Similarly, there was no significant difference in the mean tibial tunnel anteroposterior (38.63% ± 3.85% vs 37.25% ± 7.91%; $P = .67$) or mediolateral (47.75% ± 1.75% vs 46.88% ± 1.36%; $P = .28$) position. This femoral tunnel positioning was similar to the intended and actual tunnel positioning of 221 high-volume ACL surgeons.[27]

ACL Strain

There were no meaningful differences in strain among the different regions of the ACL or ACL grafts for any of the loading conditions or at any flexion angle (see Supplemental Tables S1-S3 for related data). With internal rotation and pivot-shift testing protocols, there was no significant difference in the mean ACL strain between the CFT and RFT groups in either the native or the reconstructed states at any flexion angle (Figure 4 and Table 1). In response to the anterior translation load, there was a significant difference in the mean strain between the native and reconstructed states at 60° of knee flexion independent of the type of reconstruction ($P = .048$; partial $\eta^2 = 0.251$) (Table 1 and Figure 4A). This was not seen for other flexion angles in response to anterior translation load.

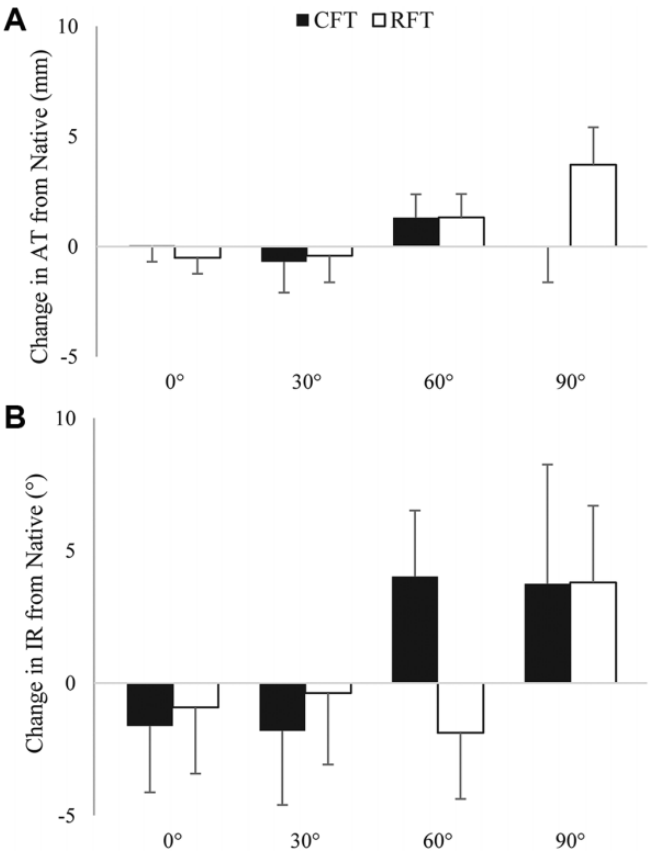

Figure 5. Change in (A) anterior translation (AT) and (B) internal rotation (IR) in response to the respective loading protocols between the native and reconstructed states for each reconstruction type. CFT, cylindrical femoral tunnel; RFT, rectangular femoral tunnel.

Knee Kinematics

For knee kinematics, in response to the isolated anterior translation load and internal rotation moment, there were no significant differences in anterior translation or internal rotation when comparing the RFT and CFT ACLR groups in the native and reconstructed states at any flexion angle (Table 2 and Figure 5). With respect to the simulated pivot-shift loading protocol, there were no significant differences in anterior translation, internal rotation, or valgus rotation between the CFT and RFT ACLRs for either the native or the reconstructed states at any flexion angle (Table 3 and Figure 6).

TABLE 3
Anterior Translation, Internal Rotation, and Valgus Rotation in Response to Simulated Pivot Shift Between the CFT and RFT Groups by Native and Reconstructed State Across Flexion Angles[a]

Variable	Native State	Reconstructed State	*P* Value (ES)
Anterior translation, mm			
0° of flexion			
CFT	3.5 ± 2.8 (1.8-5.1)	2.4 ± 1.8 (0.8-3.9)	.28 (0.59)
RFT	2.4 ± 1.2 (0.8-4.0)	2.0 ± 2.2 (0.4-3.5)	.64 (0.23)
P value (ES)	.35 (0.49)	.69 (0.20)	
30° of flexion			
CFT	2.5 ± 2.2 (0-4.0)	2.6 ± 2.4 (0.9-4.2)	.89 (0.08)
RFT	2.6 ± 1.7 (1.1-4.2)	2.6 ± 2.0 (0.9-4.3)	.94 (0.03)
P value (ES)	.88 (0.07)	.99 (0.01)	
Internal rotation, deg			
0° of flexion			
CFT	9.1 ± 7.2 (3.6-14.6)	10.9 ± 9.7 (4.6-17.1)	.41 (0.32)
RFT	14.6 ± 7.7 (9.1-20.1)	12.0 ± 6.4 (5.8-18.3)	.24 (**1.09**)
P value (ES)	.15 (0.76)	.79 (0.14)	
30° of flexion			
CFT	16.2 ± 11.5 (7.9-24.5)	18.4 ± 10.0 (12.4-24.4)	.44 (0.70)
RFT	15.7 ± 10.3 (7.4-24.0)	15.2 ± 5.2 (9.1-24.2)	.84 (0.08)
P value (ES)	.93 (0.04)	.43 (0.40)	
Valgus rotation			
0° of flexion			
CFT	2.8 ± 2.4 (0.8-3.6)	2.0 ± 1.8 (0.8-3.1)	.79 (0.45)
RFT	1.4 ± 1.1 (0.0-2.8)	1.6 ± 1.2 (0.5-2.8)	.75 (0.20)
P value (ES)	.42 (0.41)	.65 (0.23)	
30° of flexion			
CFT	1.8 ± 1.2 (0.9-2.6)	3.0 ± 1.4 (1.6-4.3)	.11 (**0.91**)
RFT	1.2 ± 1.1 (0.4-2.1)	2.6 ± 2.1 (1.3-4.0)	.06 (**0.96**)
P value (ES)	.38 (0.46)	.72 (0.18)	

[a]Data are reported as mean ± SD (95% CI) unless otherwise indicated. Bold text indicates large pairwise Cohen δ effect size (ES). CFT, cylindrical femoral tunnel; RFT, rectangular femoral tunnel.

DISCUSSION

The main finding of this biomechanical study is that there were no differences in graft strain or knee kinematics between RFT and CFT ACLR techniques using a BTB graft during anterior translation, internal rotation, or simulated pivot-shift testing protocols across knee flexion angles. However, at 60° of knee flexion, there was a significant difference in strain between the native and reconstructed states independent of the femoral tunnel type. In addition, both reconstruction techniques were equally efficacious in the replication of native ACL kinematics and ACL strain patterns, with no differences observed between the native and reconstructed states regardless of graft type or flexion angle.

It has previously been suggested that anatomic ACLR techniques using rectangular tunnels may be more effective at restoring in vitro ACL kinematics as compared with an isometric cylindrical tunnel ACLR.[38] In a cadaveric biomechanical analysis, it was determined that during passive flexion and extension, the isometric cylindrical tunnel ACLR resulted in overconstraint of the knee in terms of reduced anterior tibial displacement relative to native knee kinematics.[38] This was especially evident at lower flexion angles. The isometric ACLR using cylindrical tunnels also demonstrated significantly increased external rotation with the knee in 0° of flexion relative to the native knee. It is possible that these differences occurred as a result of the authors applying a greater initial tension to the cylindrical BTB grafts (40 N) than to the rectangular tunnel ACLR (10 N).[38] In the current investigation, a consistent initial graft tension of 80 N was applied to both the RFT and the CFT reconstructions (reflective of our clinical practice), and there were no appreciable differences in the kinematics between graft types. Further comparisons with the current study are difficult, as our technique utilized a rectangular tunnel on the femoral side only. In addition, in the study by Suzuki et al,[38] the cylindrical tunnel surgical technique positioned the tunnels in the isometric, as opposed to anatomic, position.

The RFT ACLR technique is arguably more technically demanding to perform and requires specialized equipment. This study suggests that this may not be warranted in terms of optimizing kinematics or graft strain patterns. However, other theoretical benefits to RFT have been proposed. For example, the technique may be associated with accelerated graft healing due to maximization of the graft-tunnel interface, and it has been postulated that earlier graft revascularization and remodeling could be expected.[33] When a tibial-sided rectangular tunnel technique is

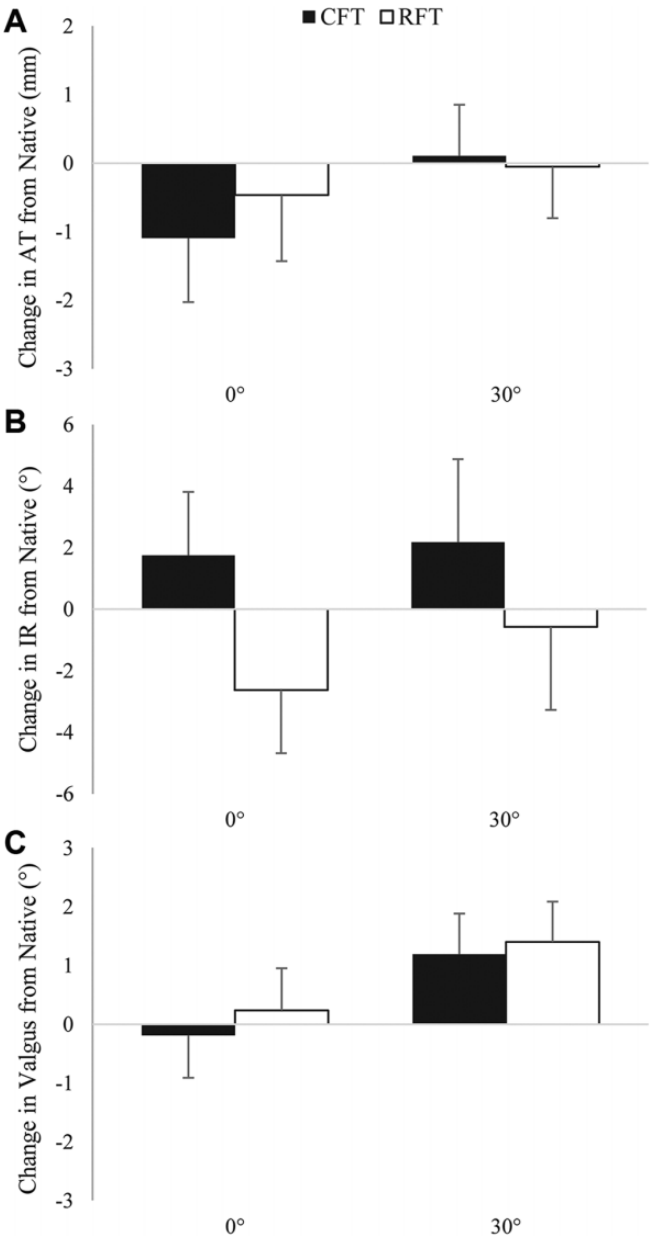

Figure 6. The change in (A) anterior translation, (B) internal rotation, and (C) valgus rotation in response to the simulated pivot shift between the native and reconstructed states for each of the reconstruction types. AT, anterior translation; CFT, cylindrical femoral tunnel; IR, internal rotation; RFT, rectangular femoral tunnel.

performed, there is minimization of surplus space adjacent to the tendinous portion of the graft in the tibial tunnel.[33] Ideally, a clinically important difference in terms of stability assessments, return-to-sports rates, patient-reported outcome measures, or graft reinjury rates would be demonstrated before widespread adoption of this technique. The present study fails to identify supportive biomechanical data, but future studies should focus on the other purported advantages of this graft type.

To our knowledge, this is the first study to noninvasively measure the strains in the ACL and ACLR grafts in response to clinically relevant loading protocols. Overall, the results suggest that both graft types demonstrated strain patterns similar to the native ACL. Although not statistically significant, there was a general trend toward reduced strain and overconstraint in the ACL reconstructed knees, regardless of reconstruction technique. This may be explained by the documented differences in BTB stiffness and strength when compared with the native ACL. The native ACL resists a maximum tensile load of approximately 2150 N and has a stiffness of 240 N/mm.[40] A 10-mm isolated BTB graft is capable of resisting tensile loads of up to 2977 N, with a stiffness of 620 N/mm.[13] Noyes et al[25] demonstrated that BTB autografts had a mean strength 159% to 168% of the native ACL and also found the BTB graft was 3 to 4 times stiffer. Interestingly, the one statistically significant difference in the current study was that the RFT and CFT ACLRs experienced significantly less strain than did the native ACL when exposed to an anterior translation load at 60° of flexion. This finding is consistent with previously reported data that determined there was a decrease in the elongation of the BTB graft at 60° when compared with the native ACL but at no other flexion angles.[39] Given that the native ACL tends to be minimally strained around 60°,[39] it is likely that there are anatomic parameters (eg, nonisometric behavior of the ACL) contributing to this finding and exacerbated by the BTB stiffness.

Another interesting finding of this study was the observation of negative strain values in both the native ACL and the reconstructed groups when exposed to isolated internal rotation, which was especially evident at higher flexion angles. In this testing environment, when strain becomes negative, the magnitude is likely not important, as the graft is not undergoing a compressive force but rather is representative of a relaxation of the structure. This observation suggests that the ACL may not be the primary structure responsible for controlling internal rotation in the absence of concomitant tibial anterior subluxation. This is supported by the finding that no negative strain values were seen in response to the simulated pivot shift that utilized a combination of loads in either the native or the ACL reconstructed state. This agrees with the findings of other biomechanical studies that have highlighted the role of the lateral knee structures, namely the iliotibial band and anterolateral complex, in controlling internal rotation, especially at higher flexion angles.[19]

There are limitations to this biomechanical study. This study is representative of time-zero kinematics, and as such, this cadaveric model does not consider the important biological factors (eg, bone incorporation) that have a role in ACLR outcomes. In addition, we only used the rectangular tunnel on the femoral side and implemented a traditional cylindrical tunnel on the tibial side. While this could have affected the placement and function of the graft, this technique is what we have been using in the clinical environment because of the ease of passage of the graft, and we believe the desirable position of the tendon on the tibial bone block can be achieved using rotation of the dowel. We also wanted to

reduce trauma to the graft during passage through the tibial tunnel, which could potentially affect bead placement. However, this decision makes it difficult to determine any potential benefits of both femoral and tibial rectangular tunnels during ACLR, including maximization of graft-tunnel wall contact within the tibial tunnel.[31] We also did not perform kinematic testing after removal of the native ACL; however, we used similar methodology to previous studies that have validated the injury model, demonstrating kinematics consistent with an ACL-deficient knee.[37] In addition, our interest was not to validate the efficacy of reconstruction compared with the injured state but instead to compare the strain between the native and reconstructed states. Finally, because of the relatively small sample size, it is possible that the investigation was underpowered to detect small differences between reconstruction techniques, particularly in relation to regional strain measurements.

CONCLUSION

In this time-zero biomechanical environment, similar graft strains and knee kinematics were achieved using RFT and CFT anatomic ACLRs using BTB autograft. Both techniques were found to be equally effective in restoring the native ACL state, with no differences observed between the intact or reconstructed states regardless of graft type. There are other potential benefits of RFT ACLR that were not evaluated in this study; however, these data suggest that in terms of knee kinematics and graft strain, there is no benefit to performing the more technically challenging RFT as compared with a standard CFT ACLR.

Supplemental material for this article is available at http://journals.sagepub.com/doi/suppl/10.1177/23259671211009523.

REFERENCES

1. Aglietti P, Giron F, Cuomo P, Losco M, Mondanelli N. Single-and double-incision double-bundle ACL reconstruction. *Clin Orthop Relat Res*. 2007;454(1):108-113.
2. Bedi A, Weber AE, Trasolini NA, et al. Does bone plug and graft orientation (inferior versus posterior) alter native femoral footprint coverage in bone patellar tendon bone anterior cruciate ligament reconstruction? *Arthroscopy*. 2020;36(7):1875-1881.
3. Bernard M, Hertel P. Intraoperative and postoperative insertion control of anterior cruciate ligament-plasty: a radiologic measuring method (quadrant method). *Unfallchirurg*. 1996;99(5):332-340.
4. Blokker A. Development and assessment of a micro-CT based system for quantifying loaded knee joint kinematics and tissue mechanics. Master's thesis. University of Western Ontario; 2018.
5. Blokker A, Getgood A, Curiale N, et al. Development and assessment of a microcomputed tomography compatible five degrees-of-freedom knee joint motion simulator. *J Biomech Eng*. 2019;141(10):101006.
6. Blokker AM, Getgood A, Nguyen D, Holdsworth DW, Burkhart TA. Insertion of small diameter radiopaque tracking beads into the anterior cruciate ligament results in repeatable strain measurement without affecting the material properties. *Ann Biomed Eng*. 2021;49(1):98-105.
7. Blokker AM, Getgood AM, Nguyen D, Burkhart TA, Holdsworth DW. Accuracy and precision of image-based strain measurement using embedded radiopaque markers. *Med Eng Phys*. Published online May 14, 2021. doi:org/10.1016/j.medengphy.2021.05.005
8. Buoncristiani AM, Tjoumakaris FP, Starman JS, Ferretti M, Fu FH. Anatomic double-bundle anterior cruciate ligament reconstruction. *Arthroscopy*. 2006;22(9):1000-1006.
9. Buscayret F, Temponi EF, Saithna A, Thaunat M, Sonnery-Cottet B. Three-dimensional CT evaluation of tunnel positioning in ACL reconstruction using the single anteromedial bundle biological augmentation (SAMBBA) technique. *Orthop J Sports Med*. 2017;5(5):2325967117706511.
10. Carmichael JR, Cross MJ. Unnecessary complication? *Arthroscopy*. 2009;25(2):219-220.
11. Cha PS, Brucker PU, West RV, et al. Arthroscopic double-bundle anterior cruciate ligament reconstruction: an anatomic approach. *Arthroscopy*. 2005;21(10):1275.e1-1275.e8.
12. Chambat P, Guier C, Sonnery-Cottet B, Fayard JM, Thaunat M. The evolution of ACL reconstruction over the last fifty years. *Int Orthop*. 2013;37(2):181-186.
13. Cooper DE, Deng XH, Burstein AL, Warren RF. The strength of the central third tendon graft: a biomechanical study. *Am J Sports Med*. 1993;21(6):818-824.
14. Fernandes TL, Morais Fonseca Martins NM, de Andrade Watai F, Neto CA, Pedrinelli A, Hernandez AJ. 3D computer tomography for measurement of femoral position in ACL reconstruction. *Acta Ortop Bras*. 2015;23(1):11-15.
15. Fu FH, Karlsson J. A long journey to be anatomic. *Knee Surg Sport Traumatol Arthrosc*. 2010;18(9):1151-1153.
16. Gill TJ. Editorial commentary: graft orientation in anterior cruciate ligament reconstruction—does it really matter? *Arthroscopy*. 2020;36(7):1882-1883.
17. Grood ES, Suntay W. A joint coordinate system for the clinical description of three-dimensional motions: application to the knee. *J Biomech Eng*. 1983;105(2):136-144.
18. Hensler D, Van Eck CF, Fu FH, Irrgang JJ. Anatomic anterior cruciate ligament reconstruction utilizing the double-bundle technique. *J Orthop Sports Phys Ther*. 2012;42(3):184-195.
19. Kittl C, El-Daou H, Athwal KK, et al. The role of the anterolateral structures and the ACL in controlling laxity in the intact and ACL-deficient knee. *Am J Sports Med*. 2016;44(2):345-354.
20. Lertwanich P, Martins CAQ, Asai S, Ingham SJM, Smolinski P, Fu FH. Anterior cruciate ligament tunnel position measurement reliability on 3-dimensional reconstructed computed tomography. *Arthroscopy*. 2011;27(3):391-398.
21. Maher JM, Markey JC, Ebert-May D. The other half of the story: effect size analysis in quantitative research. *Cell Biol Educ*. 2013;12(3):345-351.
22. Mochizuki T, Fujishiro H, Nimura A, et al. Anatomic and histologic analysis of the mid-substance and fan-like extension fibres of the anterior cruciate ligament during knee motion, with special reference to the femoral attachment. *Knee Surg Sport Traumatol Arthrosc*. 2014;22(2):336-344.
23. Mochizuki T, Muneta T, Nagase T, Shirasawa SI, Akita KI, Sekiya I. Cadaveric knee observation study for describing anatomic femoral tunnel placement for two-bundle anterior cruciate ligament reconstruction. *Arthroscopy*. 2006;22(4):356-361.
24. Muneta T, Koga H, Mochizuki T, et al. A prospective randomized study of 4-strand semitendinosus tendon anterior cruciate ligament reconstruction comparing single-bundle and double-bundle techniques. *Arthroscopy*. 2007;23(6):618-628.
25. Noyes FR, Butler DL, Grood ES, Zernicke RF, Hefzy MS. Biomechanical analysis of human ligament grafts used in knee-ligament repairs and reconstructions. *J Bone Joint Surg Am*. 1984;66(3):344-352.
26. Paessler HH. Anatomic femoral plug placement of BPTB to mimic natural fiber arrangement is not new. *Arthroscopy*. 2009;25(5):567-568.
27. Robinson J, Inderhaug E, Harlem T, Spalding T, Brown CH. Anterior cruciate ligament femoral tunnel placement: an analysis of the intended versus achieved position for 221 international high-volume ACL surgeons. *Am J Sports Med*. 2020;48(5):1088-1099.

28. Samuelsen BT, Webster KE, Johnson NR, Hewett TE, Krych AJ. Hamstring autograft versus patellar tendon autograft for ACL reconstruction: is there a difference in graft failure rate? A meta-analysis of 47,613 patients. *Clin Orthop Relat Res*. 2017;475(10): 2459-2468.
29. Shen W, Jordan S, Fu F. Review article: anatomic double bundle anterior cruciate ligament reconstruction. *J Orthop Surg*. 2007; 15(2):216-221.
30. Shino K, Mae T, Tachibana Y. Anatomic ACL reconstruction: rectangular tunnel/bone–patellar tendon–bone or triple-bundle/semitendinosus tendon grafting. *J Orthop Sci*. 2015;20(3):457-468.
31. Shino K, Mae T, Uchida R, Yokoi H, Ohori T, Tachibana Y. Anatomical rectangular tunnel ACL reconstruction with a bone-patellar tendon-bone graft: its concept, indication and efficacy. *Ann Jt*. 2019;4(5):12.
32. Shino K, Nakata K, Nakamura N, et al. Rectangular tunnel double-bundle anterior cruciate ligament reconstruction with bone-patellar tendon-bone graft to mimic natural fiber arrangement. *Arthroscopy*. 2008;24(10):1178-1183.
33. Shino K, Nakata K, Nakamura N, Toritsuka Y, Nakagawa S, Horibe S. Anatomically oriented anterior cruciate ligament reconstruction with a bone-patellar tendon-bone graft via rectangular socket and tunnel: a snug-fit and impingement-free grafting technique. *Arthroscopy*. 2005; 21(11):1402.
34. Siebold R, Schuhmacher P, Fernandez F, et al. Flat midsubstance of the anterior cruciate ligament with tibial "C"-shaped insertion site. *Knee Surg Sport Traumatol Arthrosc*. 2015;23(11):3136-3142.
35. Siebold R, Śmigielski R, Herbort M, Fink C. Anatomical anterior cruciate ligament reconstruction with a flat graft using a new tunnel creation technique. *Ann Jt*. 2019;4:27.
36. Śmigielski R, Zdanowicz U, Drwięga M, Ciszek B, Ciszkowska-Łysoń B, Siebold R. Ribbon like appearance of the midsubstance fibres of the anterior cruciate ligament close to its femoral insertion site: a cadaveric study including 111 knees. *Knee Surg Sport Traumatol Arthrosc*. 2015;23(11):3143-3150.
37. Spencer L, Burkhart TA, Tran MN, et al. Biomechanical analysis of simulated clinical testing and reconstruction of the anterolateral ligament of the knee. *Am J Sports Med*. 2015;43(9):2189-2197.
38. Suzuki T, Shino K, Otsubo H, et al. Biomechanical comparison between the rectangular-tunnel and the round-tunnel anterior cruciate ligament reconstruction procedures with a bone-patellar tendon-bone graft. *Arthroscopy*. 2014;30(10):1294-1302.
39. Tohyama H, Beynnon BD, Johnson RJ, Renstrom PA, Arms SW. The effect of anterior cruciate ligament graft elongation at the time of implantation on the biomechanical behavior of the graft and knee. *Am J Sport Med*. 1996;24(5):608-614.
40. Woo S, Hollis JM, Adams DJ, Lyon RM, Takai S. Tensile properties of the human femur-anterior cruciate ligament-tibia complex: the effects of specimen age and orientation. *Am J Sports Med*. 1991;19(3): 217-225.
41. Wu G, Siegler S, Allard P, et al. ISB recommendation on definitions of joint coordinate system of various joints for the reporting of human joint motion—part I: ankle, hip, and spine. *J Biomech*. 2002;35(4): 543-548.
42. Xie X, Liu X, Chen Z, Yu Y, Peng S, Li Q. A meta-analysis of bone-patellar tendon-bone autograft versus four-strand hamstring tendon autograft for anterior cruciate ligament reconstruction. *Knee*. 2015; 22(2):100-110.